

## NATURAL CONVECTION HEAT TRANSFER ENHANCEMENT IN AIR FILLED RECTANGULAR ENCLOSURES WITH PORTIRIONS

Angam Fadel Abid

### ABSTRACT

Natural convection of an air filled partitioned rectangular enclosure is studied numerically. Top and bottom of the enclosure are adiabatic; the two vertical walls are isothermal. Two perfectly insulated baffles were attached to its horizontal walls at symmetric position. The flow is assumed to be two-dimensional. The discretized equations were solved by finite volume method. The study was performed for different values of Rayleigh numbers  $Ra$  ( $10^4 - 10^8$ ), baffles length and position  $(L_b, S_b)$  (0-0.8, 0.2-0.8) and aspect ratios of the enclosure. The effect of  $(L_b)$  and  $(S_b)$  on heat transfer and flow were addressed. Two different patterns of the flow field were observed. The first is the flow circulate in single primary vortex strangled by two trapped fluids and the second pattern is the flow consist of two vortexes separated by one trapped fluid. With increasing of  $Ra$  heat transfer rate (Nusselt number) increased and for increasing baffles length the heat transfer rate decreases. The numerical results of the values of average Nusselt number and maximum absolute stream function have been confirmed by comparing it with similar previous works using the same boundary conditions. Good agreement was obtained.

**KEY WORDS:** Natural Convection, Heat Transfer, Rectangular Enclosure, Insulated Baffles

انتقال الحرارة بالحمل الطبيعي في وسط مغلق مقسم مستطيل الشكل مملوء بالهواء

كلية الهندسة جامعة الكوفة

تم اجراء دراسته عدديه لانتقال الحرارة بالحمل الطبيعي في وسط مغلق مقسم مستطيل الشكل مملوء تكون الجدران العموديه مسخنه الى درجات حراريه مختلفه ومنتظمه والجدران الاقفيه معزوله. حاجزين معزولين تماما الى الجدران الاقفيه بمسافات متساويه. افترض ان الجريان ثنائي البعد وتم حل المعادلات باستخدام طريقة الحجوم المحدده هذه الدراسة انجزت لقيم مختلفه من عدد رايلي  $(10^4 - 10^8)$   $(L_b, S_b)$  (0-0.8, 0.2-0.8) تم دراسة تاثير التغير في طول و موقع الحواجز على معدل انتقال الحرارة. نوعان من نماذج الجريان الاول ان الجريان يدور بدوامه منفرده والنموذج الثاني يتكون من دو بينت الدراسة ان الزيادة في عدد رايلي تسبب زياده في معدل انتقال الحرارة وزيادة طول الحواجز تسبب نقصان في معدل انتقال الحرارة. تم مقارنة النتائج العدديه لعدد نسلت واكبر قيمه مطلقه لدالة الجريان مع ب جدا لهذه البحوث.

**NOMENCLATURE**

## Angam Fadel Abid

|                      |  |
|----------------------|--|
| $A$                  | aspect ratio [ $A=H/l$ ]                                   |
| $g$                  | gravitational acceleration [ $m/s^2$ ]                     |
| $H$                  | enclosure height [m]                                       |
| $l$                  | length of enclosure [m]                                    |
| $L$                  | dimensionless baffle length [ $l/H$ ]                      |
| $Nu$                 | local Nusselt number                                       |
| $p$                  | pressure [Pa]  |
| $P$                  | dimensionless pressure [ $p/H$ ]                           |
| $Pr$                 | Prandtl number (0.7) [ $\nu / \alpha$ ]                    |
| $Ra$                 | Rayleigh number [ $g \beta H^3 (T_h - T_c) / \nu \alpha$ ] |
| $s$                  | baffle position  |
| $S$                  | dimensionless baffle position [ $s/H$ ]                    |
| $S_u, \mathcal{S}_u$ | source terms   |
| $T$                  | temperature [K]  |
| $u, v$               | components of the fluid velocity [m/s]                     |
| $U, V$               | dimensionless velocity components                          |
| $u_c$                | characteristic velocity $u = \sqrt{g \beta H (T_h - T_c)}$ |
| $x, y$               | coordinate axis [m]  |
| $X, Y$               | dimensionless axes   |

## Greek Symbols

|          |  |
|----------|--|
|          | thermal diffusion coefficient [ $m^2/s$ ]                          |
|          | volumetric thermal expansion coefficient [ $k^{-1}$ ]              |
|          | fluid density [ $kg/m^3$ ]   |
| $\theta$ | dimensionless temperature [ $\theta = \frac{T - T_c}{T_h - T_c}$ ] |
| $\nu$    | kinematic viscosity [ $m^2/s$ ]                                    |
| $\psi$   | stream function  |
|          | general scalar dependent variable                                  |
|          | diffusion coefficient  |

## Subscripts

|        |                          |
|--------|--------------------------|
| $b$    | related to baffle        |
| $c$    | cold                     |
| $h$    | hot                      |
| -      | average                  |
| e.wt.b | enclosure without baffle |

## INTRODUCTION

Over the past twenty years, a revolution in electronics has been taken place. Natural convection cooling of components attached to printed circuit boards, which are placed vertically and horizontally in an enclosure, is currently of great interest to the microelectronics industry. Natural convection cooling is desirable because it doesn't require energy source, such as a forced air fan and it is maintenance free and safe. Cavities and enclosures with no obstructions in them have been studied in the past few decades. The current interest has now shifted to complex cavities and enclosures containing obstruction or a partition which has important implications in many branches of engineering particularly in microelectronics fabrication Industry [Kandaswamy and Hakeem, 2007]. Natural convection in an air filled enclosure with vertical walls that are heated and cooled while its horizontal walls are adiabatic has received a great consideration because many of the industrial applications employ this concept as a prototype. Noticeable examples include heating and ventilating of rooms, solar collector systems electronic cooling devices and cooling of nuclear reactors. In many applications for some reasons, the cavity is partitioned by attaching baffles to its

vertical and (or) to its horizontal walls. Recent studies of heat transfer and fluid flow characteristics of the partitioned enclosure have come under scrutiny both numerically and experimentally [Ambarta and Daimaruya, 2006]. In the literature, various studies have been published on the mechanism of natural convection in differentially heated cavities and enclosures with different geometrical parameters and boundary conditions [Anikumar and Jilani, 2008].

Altaç and Kurtul [Alta and Kurtul, 2007] numerically studied 2D natural convection in tilted rectangular enclosures with a vertically situated hot plate placed at the center. The plate was very thin and isothermal. The enclosure was cooled from a vertical wall only. Rayleigh numbers ranged from  $10^5$  to  $10^6$ . The flow pattern and temperature distribution were analyzed, and steady-state plate-surface-averaged Nusselt numbers were correlated. Altac and Seda [Altac and Seda, 2009] studied an air filled rectangular enclosure containing an isothermal plate which was cooled from lateral wall while other three sides were insulated. The plate and the cold walls were maintained at constant temperatures. The governing equations were solved using finite volume method coupled with SIMPLE algorithm. Rayleigh is varied from  $10^5$  to  $5 \times 10^7$ . They found that with increasing Rayleigh the heat transfer rates increased and for increasing plate length the heat transfer rate decreased by about 25%. Zimmerman and Acharya [Zimmerman, 1987] studied numerically the natural convection heat transfer in a cavity with perfectly conducting horizontal end walls and finitely conducting baffles. Results were obtained at lower Rayleigh numbers, and no flow separation in front of partial divider was noted. Acharya and Jetli [Acharya and Jetli, 1990] had numerically investigated the heat transfer and flow patterns in a partially divided differentially heated square box. Rayleigh numbers studied were in the range of  $10^5 - 10^6$ . The flow was weak in this stratified region and a tendency for flow separation behind the divider was observed. Bajorek and Llyod [Bajorek and Llyod, 1982] studied experimentally a differentially heated air filled square partitioned cavity for Rayleigh numbers ( $1.25 \times 10^5 - 2.16 \times 10^6$ ). The insulated baffle was attached to horizontal walls at positions in the middle. Non dimensional baffle length was 0.25. The effect of the baffle positions was not considered. It was found that the baffles significantly influenced the heat transfer rate and the average Nusselt numbers reduced to approximately 15% compared to the non partitioned cavity.

Jetli et al. [Jelt iand. Acharya, 1986] studied numerically a differentially heated air filled square partitioned cavity for a Rayleigh numbers ( $10^4 - 3.55 \times 10^5$ ) with three different combinations of the baffle positions. Non dimensional baffles length was fixed at 0.33. The results clearly demonstrated that the baffles positions had a significant effect on the heat transfer and flow characteristics of the fluid. For all baffles locations, the average Nusselt number was smaller than the corresponding value in a cavity without baffle. Ambarita et al. [Ambarta and Daimaruya 2006] studied numerically a differentially heated square cavity, which is formed by horizontal adiabatic walls and vertical isothermal walls. Two perfectly insulated baffles were attached to its horizontal walls at symmetric position. The study covers Rayleigh in the range ( $10^4 - 10^8$ ), non dimensional thin baffles length  $L_b$  are (0.6-0.8), non dimensional baffle positions  $S_b$  from (0.2-0.8). It was found that Nu is an increasing function of Ra, a decreasing one of baffle length and strongly depends on  $S_b$ . Dagtekin and Oztop [Dagtekin, and. Oztop 2001] numerically studied the natural convection heat transfer and fluid flow of two heated partitions in a rectangular enclosure for Rayleigh number range of 104-106. The partitions were attached to the bottom wall; the length and the location were varied while the enclosure was cooled from two walls. Nakhi and Chamkha [Dagtekin, and. Oztop 2001] numerically investigated natural convection heat transfer from an inclined heat fin attached to the hot wall of a square enclosure. In the present work we study natural convection in an air filled partitioned rectangular enclosure is studied. The enclosure is differentially heated and the baffles were attached to top and bottom walls. The baffles are thin, perfectly insulated and non dimensional baffles length  $L_b$  are varies from (0 to 0.8) and non dimensional baffles positions  $S_b$  from (0.2-0.8). The objective of this paper is to make clear the effects of the long baffles and aspect ratios of the enclosure on the flow, temperature fields and heat transfer.

**MATHEMATICAL FORMULATION**

Consider a two-dimensional rectangular enclosure as shown in **Figure 1**. The top and bottom walls of the enclosure are adiabatic and the two vertical walls have different uniform temperatures. Left and right walls are isothermal at  $T_h$  and  $T_c$  respectively. Two-thin baffles with non dimensional length perfectly insulated are attached to the top and the bottom walls. The positions of the top baffle from the right wall and the bottom baffle from the left wall are the same. The Cartesian coordinates( $x, y$ ) with the corresponding velocity components ( $u, v$ ) are as indicated in **Figure 1**.The gravity  $g$  acts normal to the  $y$ -direction. The flow is assumed to be laminar, two-dimensional, steady state condition. Under Boussinesq approximation the compressibility, radiation, heat exchange and dissipations are negligible. All of the thermal properties are constant except density in the buoyancy force. Based upon the previous assumptions and introducing the following dimensionless variables [**Kandaswamy and Hakeem, 2007**]:

$$\left. \begin{aligned} X &= \frac{x}{H}, Y = \frac{y}{H} \\ U &= \frac{u}{u_c}, V = \frac{v}{u_c} \\ P &= \frac{p}{\rho u_c^2}, \theta = \frac{T - T_c}{T_h - T_c} \end{aligned} \right\} \quad (1)$$

The governing equations for the present study will take the following forms [**Kandaswamy and Hakeem2007**]:

Continuity:

$$\frac{\partial u}{\partial x} + \frac{\partial v}{\partial y} = 0 \quad (1a)$$

X-momentum

$$\left( u \frac{\partial u}{\partial x} + v \frac{\partial u}{\partial y} \right) = -\frac{1}{\rho} \frac{\partial p}{\partial x} + \nu \left( \frac{\partial^2 u}{\partial x^2} + \frac{\partial^2 u}{\partial y^2} \right) \quad (2)$$

Y-momentum

$$\left( u \frac{\partial v}{\partial x} + v \frac{\partial v}{\partial y} \right) = -\frac{1}{\rho} \frac{\partial p}{\partial y} + \nu \left( \frac{\partial^2 v}{\partial x^2} + \frac{\partial^2 v}{\partial y^2} \right) + g \beta (T - T_c) \quad (3)$$

Energy equation

$$\left( u \frac{\partial T}{\partial x} + v \frac{\partial T}{\partial y} \right) = \alpha \left( \frac{\partial^2 T}{\partial x^2} + \frac{\partial^2 T}{\partial y^2} \right) \quad (4)$$

The dimensionless forms of the governing equations will be as follow;

$$\frac{\partial U}{\partial X} + \frac{\partial V}{\partial Y} = 0 \quad (5)$$

$$U \cdot \left( \frac{\partial U}{\partial X} \right) + V \cdot \left( \frac{\partial U}{\partial Y} \right) = -\left( \frac{\partial P}{\partial X} \right) + \text{Pr} \left[ \left( \frac{\partial^2 U}{\partial X^2} \right) + \left( \frac{\partial^2 U}{\partial Y^2} \right) \right] \quad (6)$$

$$U \cdot \left( \frac{\partial V}{\partial X} \right) + V \cdot \left( \frac{\partial V}{\partial Y} \right) = -\left( \frac{\partial P}{\partial Y} \right) + \text{Pr} \left[ \left( \frac{\partial^2 V}{\partial X^2} \right) + \left( \frac{\partial^2 V}{\partial Y^2} \right) \right] + Ra \text{ Pr } \theta \quad (7)$$

$$U \cdot \left( \frac{\partial \theta}{\partial X} \right) + V \cdot \left( \frac{\partial \theta}{\partial Y} \right) = \left[ \left( \frac{\partial^2 \theta}{\partial X^2} \right) + \left( \frac{\partial^2 \theta}{\partial Y^2} \right) \right] \quad (8)$$

The boundary conditions in dimensionless form are:

$$U = V = 0, \theta = 1 \quad \text{on the left wall}$$

$$U = V = 0, \theta = 0 \quad \text{on the right wall}$$

$$U = V = 0, \frac{\partial \theta}{\partial Y} = 0 \quad \text{on the top and bottom walls}$$

$$U = V = 0 \quad \text{on the baffles}$$

Where the velocity components are defined as:

$$U = \frac{\partial \psi}{\partial Y}, \quad V = -\frac{\partial \psi}{\partial X} \quad (9)$$

The local Nusselt number Nu is defined by [Ambarta, Kishinami and Daimaruya2006]:

$$Nu = \frac{\partial \theta / \partial X|_{x=0}}{(\theta_h - \theta_c)} dX \quad (10)$$

Resulting in the average Nusselt number as:

$$\bar{Nu} = \int_0^1 Nu dY \quad (11)$$

## NUMERICAL METHOD

Numerical solutions for the governing equations with the associated boundary conditions are obtained using finite-volume techniques. A general conservation equation form common to all governing equations may be given in Cartesian form as follow [Patankar and Spalding, 1972]

$$\frac{\partial}{\partial X_i} (\rho u_i \Phi) = \frac{\partial}{\partial X_i} \left( \Gamma \frac{\partial \Phi}{\partial X_i} \right) + S \quad (12)$$

where the general scalar  $\Phi$  stands for any one of the dependent variables under consideration. The diffusion coefficient  $\Gamma$  and the source term  $S$  in cartesian form are listed below for each governing equation [Versteeg and Malalasekera, 1995] ;

Continuity equation

$$\Phi = 1, \Gamma = 0, S = 0$$

Momentum equation in X-direction

$$\Phi = U, \Gamma = \mu, S = -\frac{\partial P}{\partial X}$$

Momentum equation in Y-direction

$$\Phi = V, \Gamma = \mu, S = -\frac{\partial P}{\partial Y} + Ra Pr \theta$$

Energy equation

$$\Phi = \theta, \Gamma = 1, S = 0$$

The numerical solution of the governing equations will be made according to the finite volume method to transform the governing equations from partial differential form to discrete algebraic form; the staggered grid system is used. This method is based on principle of dividing the flow field to a number of volume elements, each one of them is called (control volume), after that a discretization process is carried out by integrating the general conservation equation (12) over a control volume element, where this equation will be as follow;

$$a_P \Phi_P = a_E \Phi_E + a_W \Phi_W + a_N \Phi_N + a_S \Phi_S + S_u \tag{13}$$

where;

$$a_P = a_E + a_W + a_N + a_S - S_P \tag{14}$$

The source coefficients ( $S_u$  &  $S_p$ ) represent the source terms of the discrete equation and their values for each governing equation which are listed as follow:

- For the continuity equation

$$\left. \begin{aligned} S_u &= 0 \\ S_p &= 0 \end{aligned} \right\} \tag{15}$$

- For X-momentum

$$\left. \begin{aligned} S_u &= -\frac{\partial P}{\partial X} \\ S_p &= 0 \end{aligned} \right\} \tag{16}$$

- For Y-momentum

$$\left. \begin{aligned} S_u &= -\frac{\partial P}{\partial Y} + Ra \ Pr \ \theta \\ S_p &= 0 \end{aligned} \right\} \tag{17}$$

- For energy equation

$$\left. \begin{aligned} S_u &= 0 \\ S_p &= 0 \end{aligned} \right\} \tag{18}$$

The discretized algebraic equations are solved by the SIMPLE algorithm. Relaxation factors of about (0.01–0.1) are used for all dependent variables, convergence is measured in terms of the maximum change in each variable during iteration under the following condition:

$$\frac{\sum_{i,j} |\phi_{i,j}^n - \phi_{i,j}^{n-1}|}{\sum_{i,j} |\phi_{i,j}^n|} \leq 10^{-5}$$

where  $\phi$  stands for either  $U, V, \theta$  and  $n$  denotes the iteration step.

In order to determine the proper grid size for this study, a grid independence test is conducted for the values of Ra ( $10^4, 10^6, 10^8$ ) and at  $L_b=0.6, S_b=0.4$ . Five different grid densities 40\*40, 60\*60, 80\*80, 100\*100, 120\*120 are taken. The maximum value of absolute stream function and average Nu are selected as the monitoring variables for the grid independence study. The results are presented in Fig.(2), and comparison of predicted  $|\psi_{max}|$  and  $Nu$  values among five different cases suggests that the three grid distributions 80\*80, 100\*100, 120\*120 gives nearly

identical results. Considering both the accuracy and the computational time the following calculations were all performed with a 80\*80 grid system.

## RESULTS AND DISCUSSIONS

Natural convection at low Prandtl number (0.7), corresponding to an air is investigated numerically in the presence of a two perfectly insulated baffles which are attached to horizontal walls of the rectangular enclosure at symmetric positions and at different aspect ratios ( $A=1,2$ ). The computations are carried out for a wide range of Rayleigh number varying from  $10^4$  to  $10^8$ . The results are depicted as streamlines, isotherms plots and other figures. The rate of heat transfer across the enclosure is calculated in terms of average Nusselt number  $N\bar{u}$ . **Figure 3** shows the streamlines and isotherms for square enclosure without baffles at different Ra. **Figure 3 (a)** shows that the streamlines, it can be seen that the flow consists of single cell filling the entire enclosure and causing circulatory motion of the fluid because of buoyancy effects. The rise of fluid due to heating on the left wall and consequent falling of the fluid on the right wall creates a clockwise rotating vortex referred to as the primary vortex. As Ra increases the streamlines become closer to the vertical walls, this suggests that the flow moves faster as natural convection is intensified. The maximum absolute value of stream function can be viewed as a measure of the intensity of natural convection in the enclosure. As (Ra) increases the maximum absolute value of the stream function increases. This means, that the intensity of natural convection in the enclosure increases as Ra increases. **Figure 3 (b)** represents the isotherms, as Ra increases the temperature levels will increase gradually where the hot fluid rises up along the left-hand side hot wall and descends along the right-hand side cold wall because of the buoyancy effect [Altac and.Seda, 2009].

Flow and temperature fields for the square enclosure with baffles are presented in **Figure 4**. In this figure, the non-dimensional baffle positions  $S_b$  are taken (0.2-0.6), and the non-dimensional baffle length  $L_b$  varied from 0.2 to 0.6 at different Ra. The bottom baffle is on the hot side and the top baffle is on the cold side of the enclosure. It can be seen the flow field can be divided into two patterns. The first pattern is the fluid circulates and creates a large clockwise primary vortex strangled by the baffles [Ambarta, Kishinami, Daimaruya, Saitoh, Takahashi and Suzuki, 2006], [Altac and.Seda, 2009]. The second pattern is the fluid separated into two different vortexes. This pattern can be seen when Ra increases. As the intensity of natural convection increases, the primary vortex starts dividing into two vortex, cold vortex and hot vortex in order to satisfy the continuity. These two vortexes are separated by one trapped fluid which is stagnant between the two baffles. **Figure 4 (a) and (b)** shows streamlines at low Ra ( $10^4$ ) and  $L_b < 0.5$  the natural convection creates a single vortex in the entire enclosure. These vortexes are strangled by two trapped fluids, the hot trapped fluid exists between the bottom baffle and the hot wall and the cold trapped fluid exist between top baffle and cold wall. The primary vortex starts dividing into two vortex, cold vortex and hot vortex, When  $L_b$  and  $S_b > 0.5$ . These two vortexes are separated by one trapped fluid which is stagnant between the two baffles because natural convection is too weak to make the trapped fluids moving. When Ra increases ( $10^6$ ) and  $L_b < 0.5$ , the streamlines become more closer to the vertical wall, producing strong boundary layer effects on the isothermal walls, and the flow remains unicellular. When  $L_b > 0.5$  and  $S_b < 0.5$ , there are two vortexes in the enclosure and the trapped fluid exists between the two baffles, because when Ra increases the natural convection increases and make the trapped fluid moving faster. For  $S_b > 0.5$ , the two vortexes are combine to become a primary vortex because the spaces between each baffle and the nearest wall are wide enough, and some of the trapped fluid exists in hot and cold side. The corresponding isothermal contours are presented in **Figure 4 (c) and (d)**. The isotherms shows slight deviation from the pure conduction case with the contour lines becoming skewed at low Ra [Ambarta, Kishinami, Daimaruya, Saitoh, Takahashi, and Suzuki, 2006]. At high Ra the isotherms becomes almost horizontal between the two baffles and dense of this lines are established

at the bottom left and top right of the enclosure due to faster moving fluid and the separation of the primary vortex.

**Figure 5 (a) and (b)** represent the streamlines for  $A=2$ ,  $S_b$  (0.2-0.6) and  $L_b$  (0.2-0.6) at different Ra. At low Ra ( $10^4$ ), the main circulation encircles the enclosure formation a single vortex like square enclosure, the only difference is in the dimensions of the trapped fluid and the maximum value of absolute stream function. With increasing Ra and when  $L_b$  and  $S_b < 0.5$  the inner roll within the main vortex between the baffles develops and gains strength and will be distorted. When  $L_b > 0.5$  the unicellular circulation inside the main vortex is broken up into two rolls and concentration of streamlines near the baffles because the natural convection is enough to make all of the trapped fluids flow. When  $S_b > 0.5$  the flow consists of one vortex strangled by two trapped fluids, hot trapped fluid exists between the top baffle and the hot wall and the cold trapped fluid exists between the bottom baffle and the cold wall. **Figure 5 (c) and (d)** shows the contour lines of the temperature distribution. At low Ra, the isotherms are almost straight lines like square enclosure. The increase in Ra results in a significant horizontal temperature gradient between the baffles and producing closer isotherms in the trapped fluid because the temperature difference on vortex areas is small due to fluid circulation but it is high on the trapped fluid. The trapped fluids block the convection heat transfer from hot wall to cold wall and conduction heat transfer are only considered.

For square enclosure, the average Nu is plotted in **Figure 6** as a function of Ra and for different  $L_b$  (0.3, 0.7) and  $S_b$  (0.2, 0.4, 0.6, 0.8). The average Nusselt number  $\overline{Nu}$  for the enclosure without baffle is also presented in this figure by a dashed line as a reference. This figure shows the appearance of  $\overline{Nu}$  lines pattern is similar with each other, the only differences are in the quantity of  $\overline{Nu}$ . This is because the length of the baffles changes the quantity of  $\overline{Nu}$ . With increasing baffle length the average Nu decreases for all values of Ra, because the length of trapped fluid between the two baffles is decreased. The  $(\overline{Nu})$  increases with increasing Ra due to increased temperature gradients along the hot and cold walls.  $(\overline{Nu})$  for case  $S_b < 0.5$  are lower than the cases when  $S_b > 0.5$ . This is because  $\overline{Nu}$  is trapped fluid's dimension dependent that increases as its width increases but decreases as its length increases. Fig(6.a) shows the case with  $L_b$  (0.3). For  $S_b$  (0.2),  $\overline{Nu}$  is decreased by 22.7% at  $Ra=10^4$  and by 36.3% at  $Ra=10^8$ , the average is 29.5%. For  $S_b$  (0.6) at  $Ra=10^4$ ,  $\overline{Nu}$  is decreased by 31.4% and is 27.1% at  $Ra=10^8$ , the average is 29.2%. These values suggest that the case with  $S_b$  (0.2) blocks the heat transfer rate more effectively than with  $S_b$  (0.6) because the width of the trapped fluid becomes smaller. For  $L_b = 0.7$  and  $S_b = 0.2$  (Fig. (6.b)), at  $Ra=10^4$ ,  $\overline{Nu}$  is decreased by 33.4% and at  $Ra=10^8$ , it is 48.5%, the average 40.9%, while at  $S_b$  (0.6), at  $Ra=10^4$   $\overline{Nu}$  is decreased by 35.2% and at  $Ra=10^8$ , it is 31%, the average 33.1%. These values suggest when increasing baffles length blocks the heat transfer rate more effectively, because the uncovered vertical walls are decreased with increasing baffles length, and longer uncovered areas reveal higher  $\overline{Nu}$ , since the heat transfer rate correlates with natural convection on the uncovered vertical walls.

**Figure 7** represents the variation of  $\overline{Nu}$  for  $A=2$  as a function of Ra and for different parameters. For  $L_b = 0.3$  and  $S_b = 0.2$  (**Figure 7 (a)**),  $\overline{Nu}$  is decreased by 18.8% at  $Ra=10^4$ , and at  $Ra=10^8$ , it is 43.9%, the average 11.4%, while at  $S_b$  (0.6), at  $Ra=10^4$   $\overline{Nu}$  is decreased by 22.8% and at  $Ra=10^8$ , it is 4.2%, the average 13.5%. For  $L_b = 0.7$ ,  $\overline{Nu}$  is decreased by 53.1% for  $S_b = 0.2$ , and  $Ra=10^4$ , and is 41.6% for  $Ra=10^8$ . For  $S_b = 0.6$ ,  $\overline{Nu}$  is decreased by 36.3% for  $Ra=10^4$ , and 25.8% for  $Ra=10^8$ . **Figure 8 (a)** represent the variation of Nu with  $L_b$  at  $S_b$  (0.2) it can be seen with increasing the baffle length the average Nu is decreased. **Figure 8 (b)** represent the variation of  $\overline{Nu}$  with  $S_b$  at  $L_b$  (0.6). It can be seen with increasing  $S_b$ , the average Nusselt number will be

increasing until ( $S_b=0.6$ ), because the area of the trapped fluid is increasing and  $Nu$  is trapped fluid's dimension dependent that increases as its width increases.

To exhibit the reliability of the presented results, the variation of average Nu with Ra at ( $L_b = 0.6, S_b = 0.6, A = 1$ ) were compared with Ambarita et al. [Ambarta, Kishinami, Daimaruya, Saitoh, Takahashi and Suzuki, 2006] at the same conditions as shown in Figure 9 (a), where it is clear the similarity in Nu behavior at high Ra with mentionable study, but there is small difference between these values because of different grid sizes used and round offs in the computational process. Another comparison was made with the same work for maximum absolute stream function as shown in Figure 9 (b). The comparison shows a good agreement.

## CONCLUSIONS

In this study heat transfer enhancement of air filled partitioned rectangular enclosure for various pertinent parameters like baffle length and position, Rayleigh number and aspect ratios of the enclosure. The enclosure was performed by vertical isothermal walls and adiabatic horizontal walls. Two thin insulated baffles were attached to its horizontal walls at symmetric position. The main conclusions of the present study are:

- 1-The flow field can be divided into two patterns, The first is the flow circulate and creates a primary vortex strangled by two trapped fluids and the second pattern is the flow consist of two vortices separated by one trapped fluids.
- 2-At low Ra and ( $L_b, S_b$ )  $< 0.5$ , the flow circulate as a single primary vortex and at high Ra and  $L_b > 0.5$  the flow separated in two vortices for square enclosure.
- 3-For rectangular enclosure, at low Ra and ( $L_b, S_b$ )  $> 0.5$  the flow consist of two vortices separated by one trapped fluid, but at high Ra the flow consist of primary vortex with inner roll is broken up into two rolls.
- 4-The average Nusselt number increases as Rayleigh number increases.
- 5-As the baffles length  $L_b$  increases the average Nusselt number will be decreased.
- 6-With increasing the baffles position  $S_b$ , the average Nusselt number increases until ( $S_b = 0.6$ )

## REFERENCES

- 1-P.Kandaswamy, J.Lee, A.K.Hakeem, "Natural convection in a square cavity in the presence of heated plate", Nonlinear Analysis: Modeling and Control, Vol.12, No.,2,203-212,2007.
- 2-H.Ambarta, K.Kishinami, M.Daimaruya, T.Saitoh, H.Takahashi, and J.Suzuki, "Laminar natural convection heat transfer in an air filled square cavity with two insulated baffles attached to its horizontal walls", J. Thermal Science and Eng., Vol.,14, No.,3,2006.
- 3-S.H.Anikumar, and G.Jilani, "Natural convection heat transfer enhancement in a closed cavity with partition utilizing nano fluids", Proc.of the World Congress on Eng., Vol.,II, July 2-4,2008.
- 4-Z.Ata, and O, Kurtul, "Natural convection in tilted rectangular enclosures with a vertically situated hot plate inside", J. Applied Thermal Engineering, Vol. 27, pp.1832-1840, 2007.
- 5-Z.Altac, and K.Seda, "Natural convection heat transfer from a thin horizontal isothermal plate in air filled rectangular enclosures", J. of Thermal Science and Technology, 29, 1, 55-65, 2009.
- 6-E. Zimmerman, S.Acharya, "Free convection heat transfer in a partially divided vertical enclosure with conducting end walls", Int.J. HMT, Vol.30 (2), , pp.319-331, 1987.
- 7- S.Acharya, R.Jetli, "Heat transfer due to buoyancy in a partially divided square box", Int. J. Heat Mass Transfer, 33 (5), pp.931-942,1990.

## **Angam Fadel Abid**

8-S.Bajorek, and J.Lloyd,"Expermental investigation of natural convection in partitioned enclosures",J.Heat Transfer,104,527-532,1982.

9- R.Jelti,S.Acharya,E.Zimmerman"Influnce of baffle location on natural convection in a partially divided enclosure"Numerical Heat Transfer,10,521-536,1986.

10-I.Dagtekin, and H.F. Oztop, "Natural convection heat transfer by heated partitions", Int. Commun Heat Mass Transfer 28, pp. 823-834, 2001.

11- B.A-Nakhi, andA.J. Chamkha., "Effect of length and inclination of a thin fin on natural convection in a square enclosure",J. Numer Heat Transfer, Part A 50, pp.389- 407, 2006.

12-Patankar and Spalding, "A calculation procedure for heat, mass, and momentum transfer in three-dimensional parabolic flow," Int. J. Heat Mass Transfer, Vol. 15, PP. 1787-1805, 1972.

13- H. K.Versteeg, and W.Malalasekera,"An introduction to computational fluid dynamics the finite volumes method", Longman Group Ltd, 1995.

NATURAL CONVECTION HEAT TRANSFER ENHANCEMENT IN AIR FILLED RECTANGULAR ENCLOSURES WITH PORTIRIONS

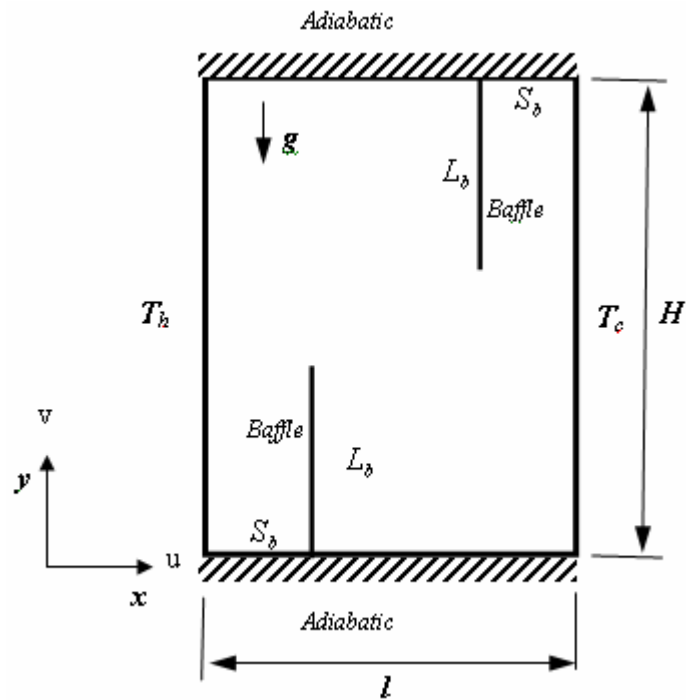


Figure 1 Physical model and coordinate system.

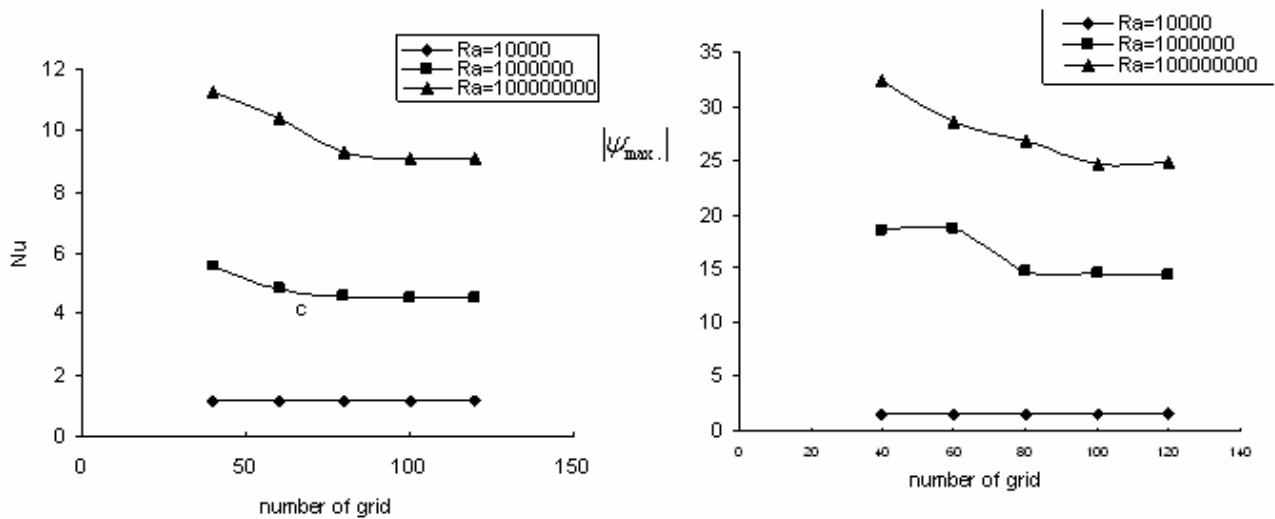
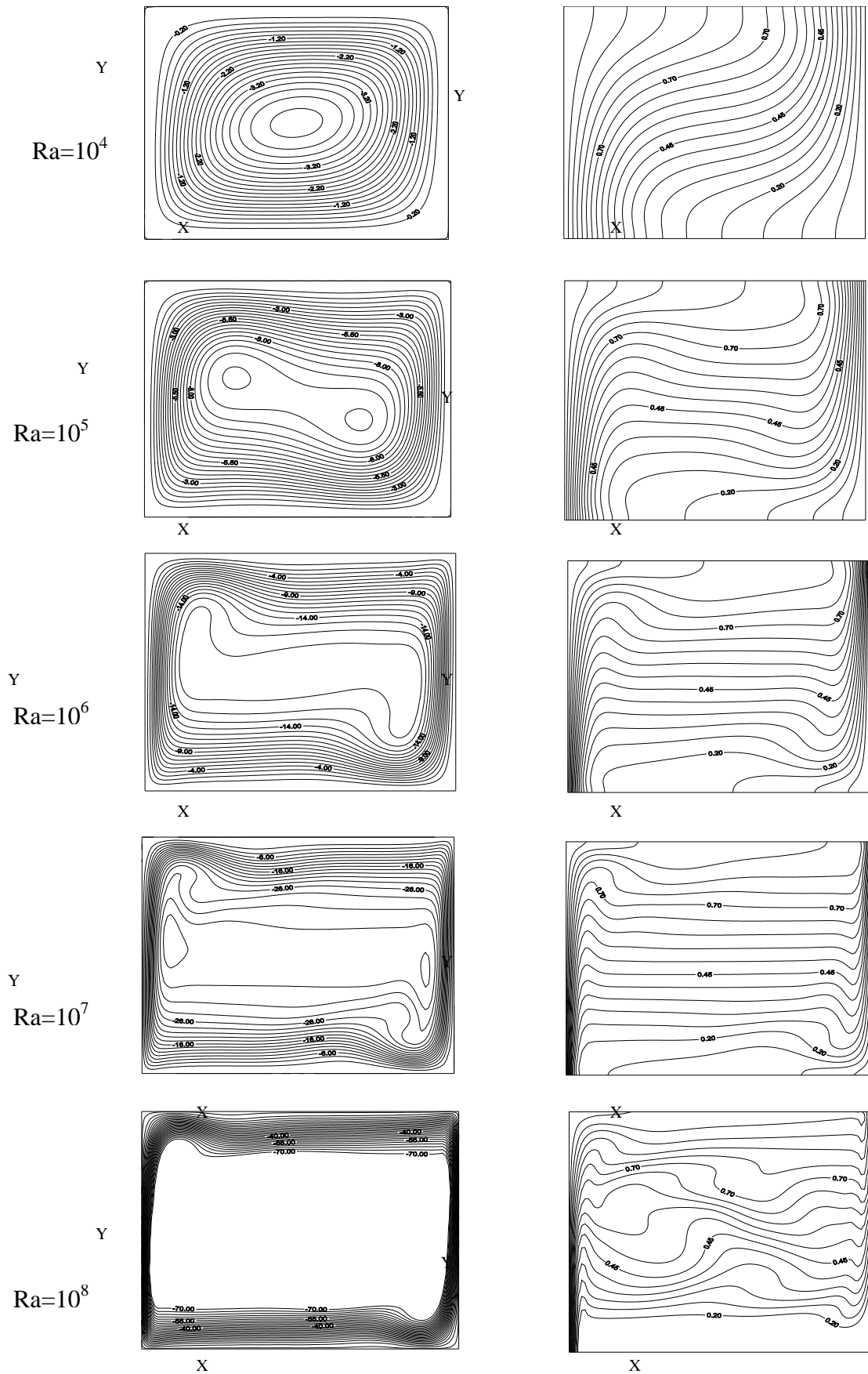
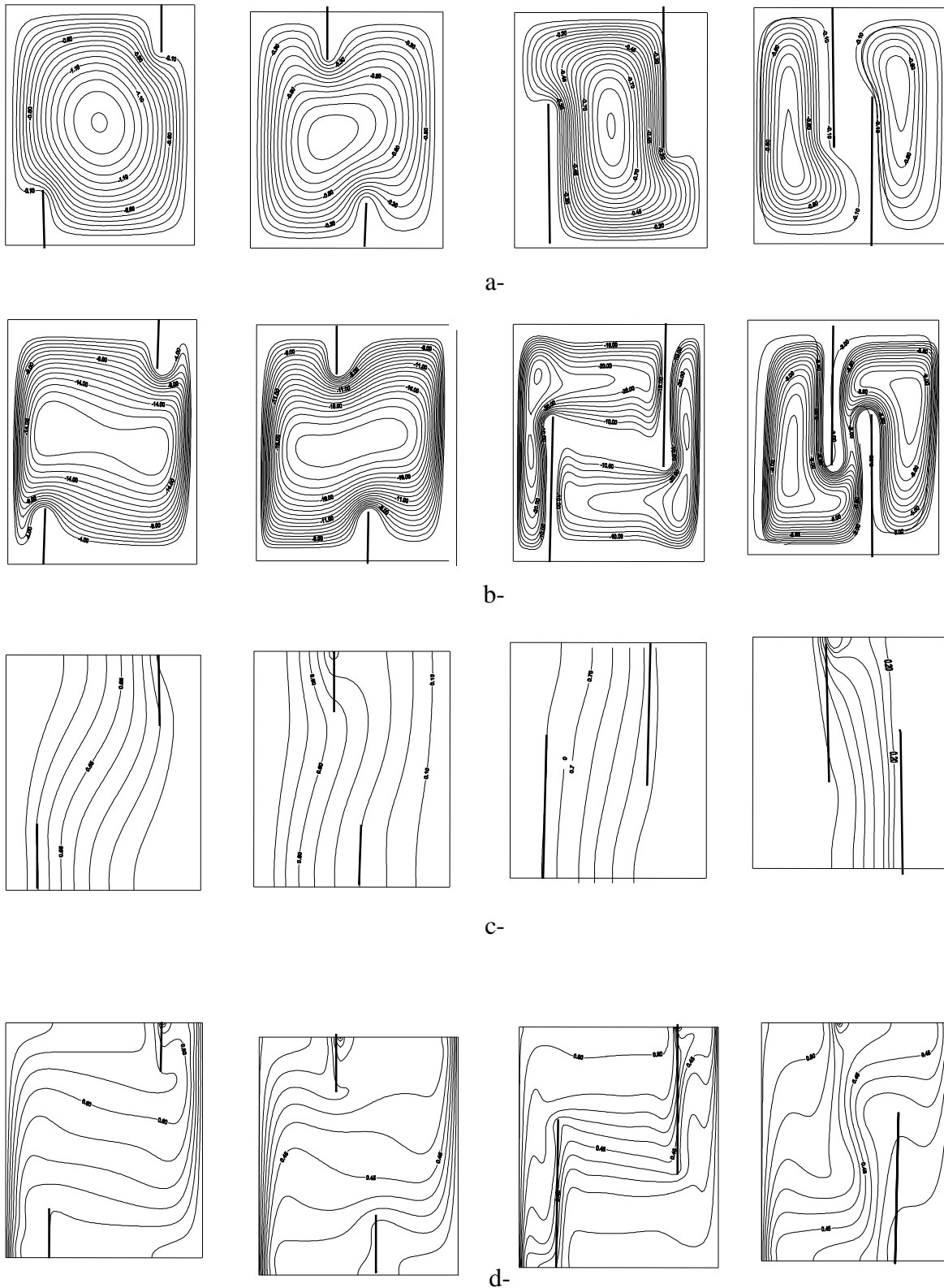


Figure 2 Variation of Nusselt number and maximum absolute stream function with the number of grid points for different Rayleigh number.



**Figure 3** Streamlines and isothermal plot for natural convection in square enclosure without baffles, a-streamlines, b-isothermal

NATURAL CONVECTION HEAT TRANSFER ENHANCEMENT IN AIR FILLED RECTANGULAR ENCLOSURES WITH PORTIRIONS



**Figure 4** Streamlines and isothermal plot in square enclosure ,a,c-  $Ra=10^4$ ,b,d- $Ra=10^6$ :the first column  $S_b=0.2, L_b=0.2$ , second column  $S_b=0.8, L_b=0.2$ ,third column  $S_b=0.2, L_b=0.6$ ,fourth column  $S_b=0.6, L_b=0.6$

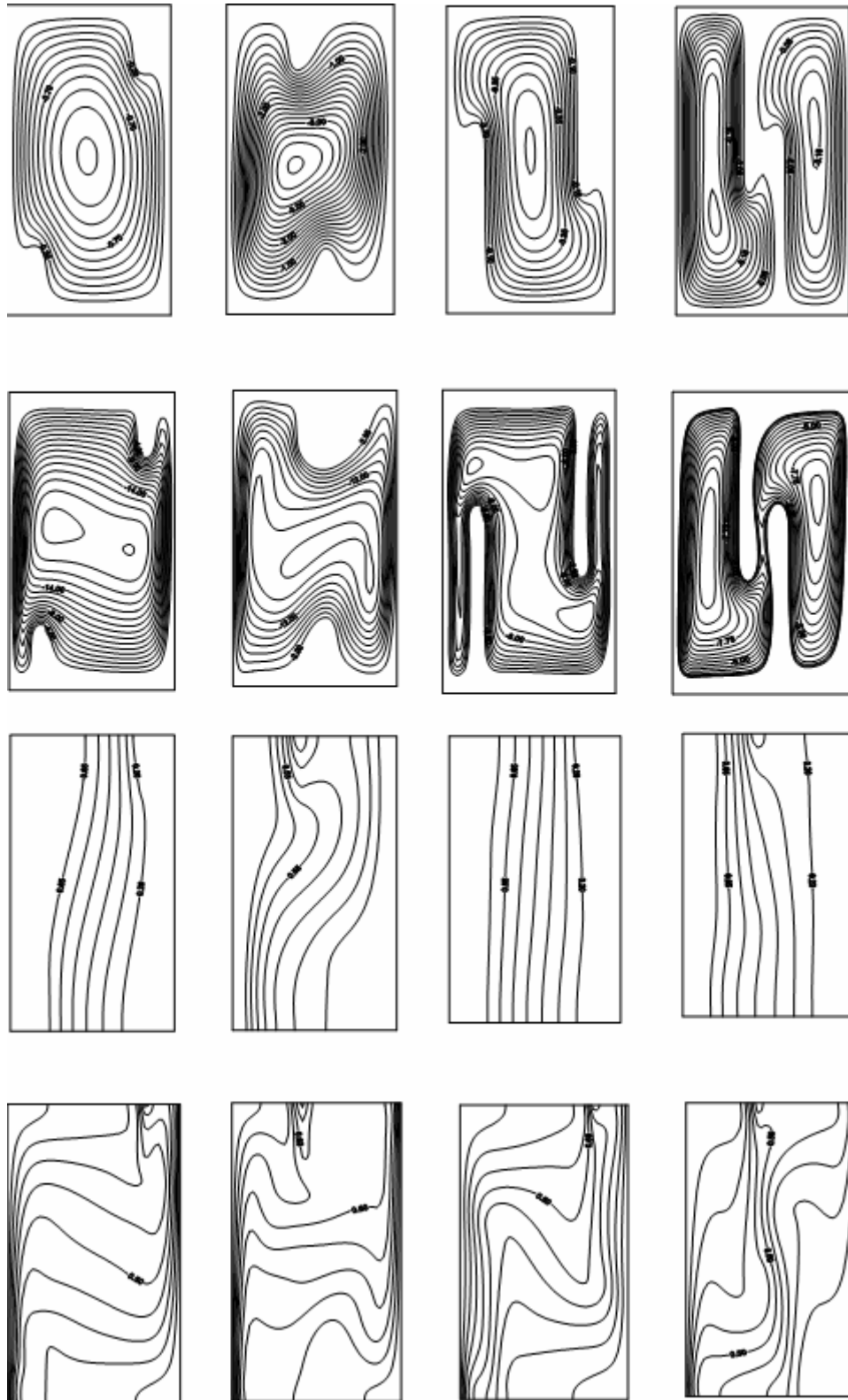
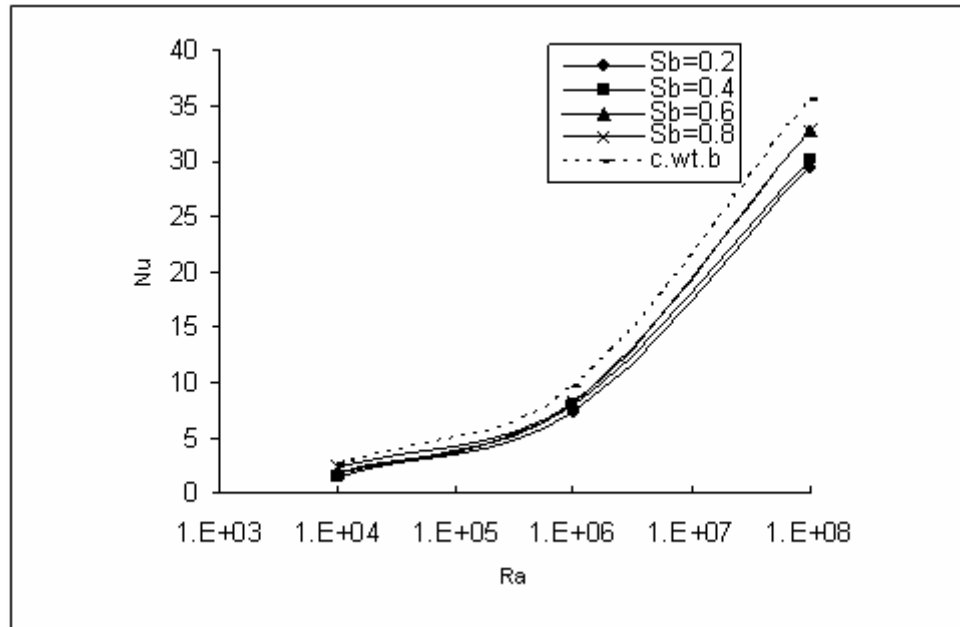
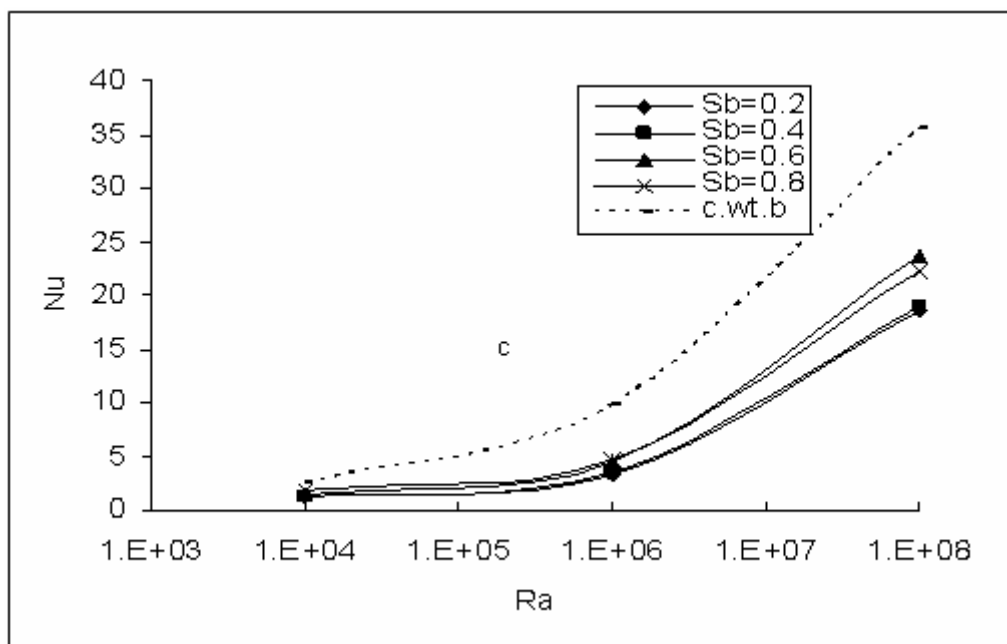


**Figure 5** Streamlines and isothermal plot for  $A=2$  ,  $a,c-Ra=10^4$ ,  $b,d-Ra=10^6$ , the first column  $S_b=0.2, L_b=0.2$ , second column  $S_b=0.6, L_b=0.2$ , third column  $S_b=0.2, L_b=0.6$ , fourth column  $S_b=0.6, L_b=0.6$

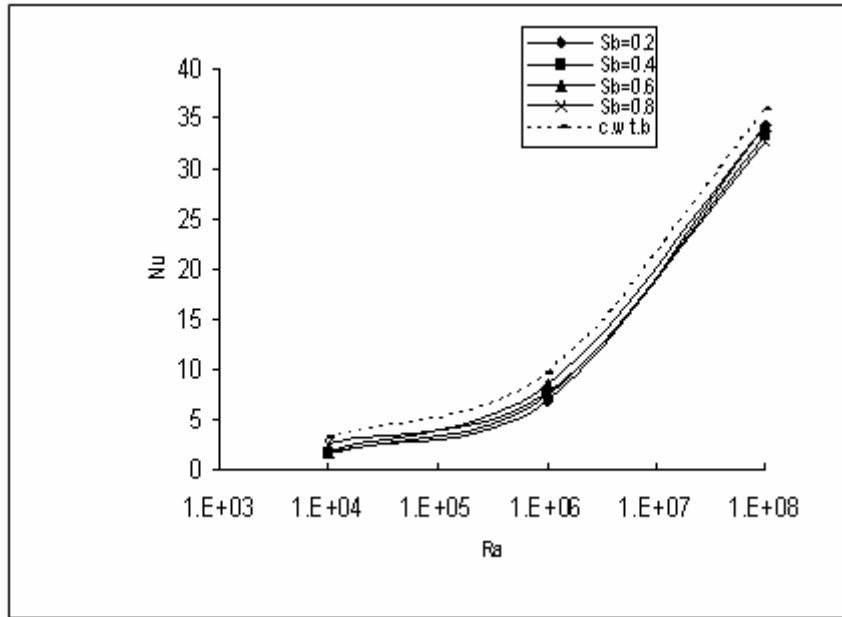


(a)

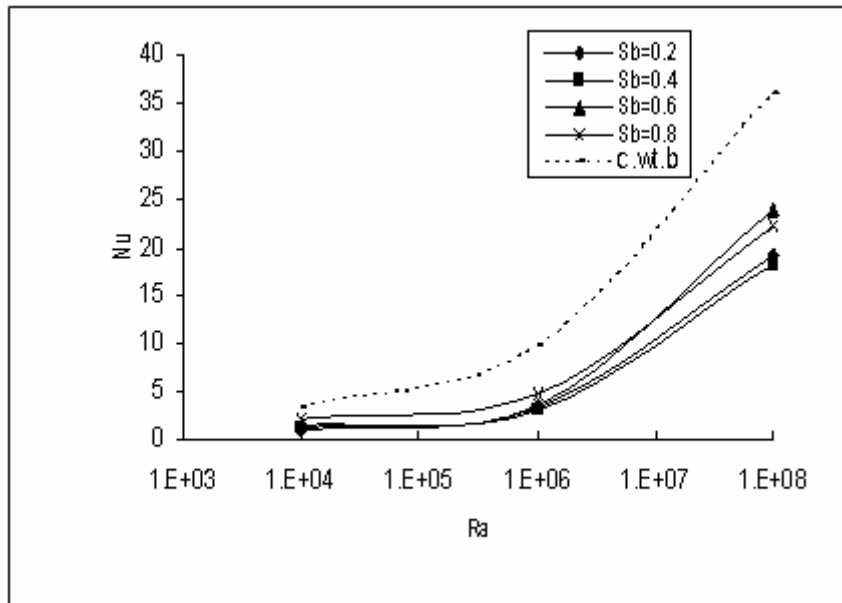


(b)

**Figure 6** Variation of Nusselt number with Rayleigh number with  $S_b$  as a parameter for  $A=1$ ; (a)  $L_b=0.3$ , (b)  $L_b=0.7$



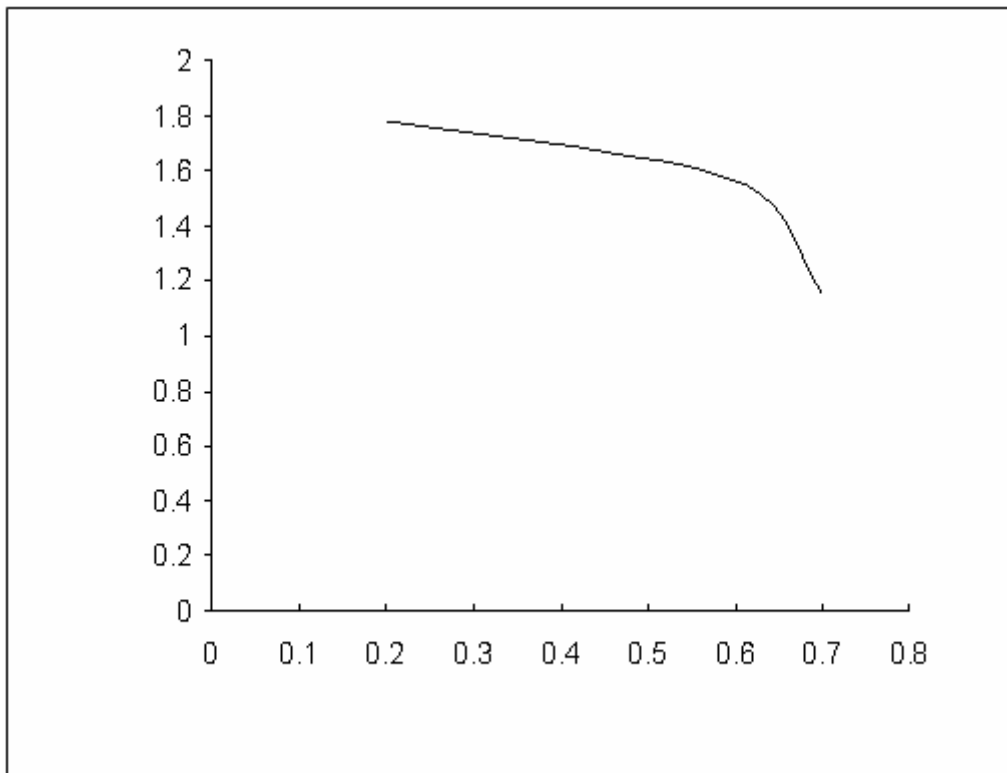
(a)



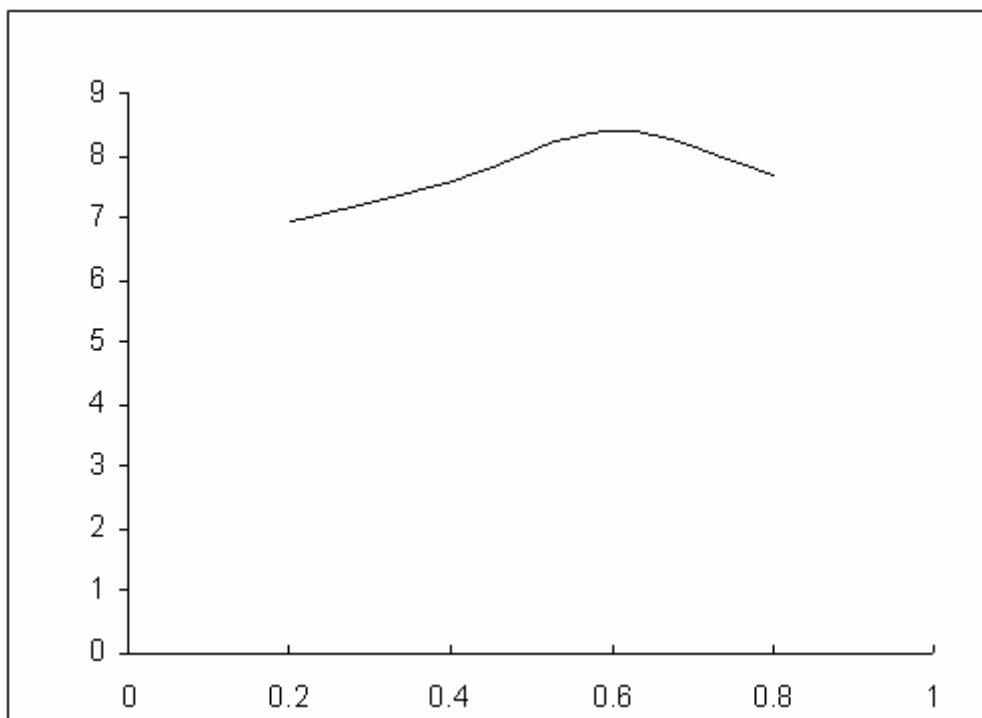
(b)

**Figure 7** Variation of Nusselt number with Rayleigh number with Sb as a parameter for A=2; (a) Lb=0.3, (b) Lb=0.7

NATURAL CONVECTION HEAT TRANSFER ENHANCEMENT IN AIR FILLED RECTANGULAR ENCLOSURES WITH PORTIRIONS

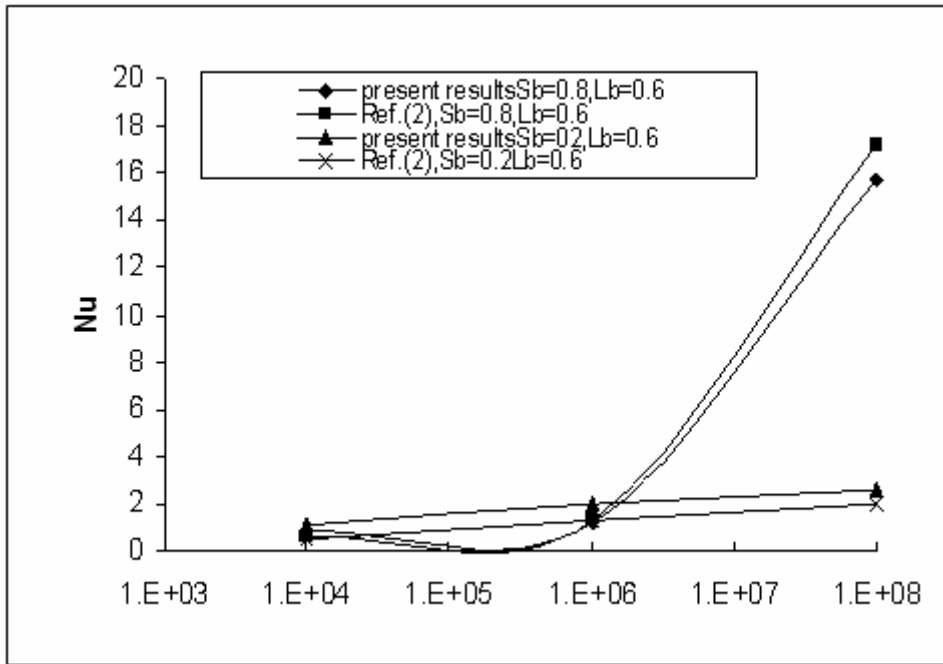


(a)

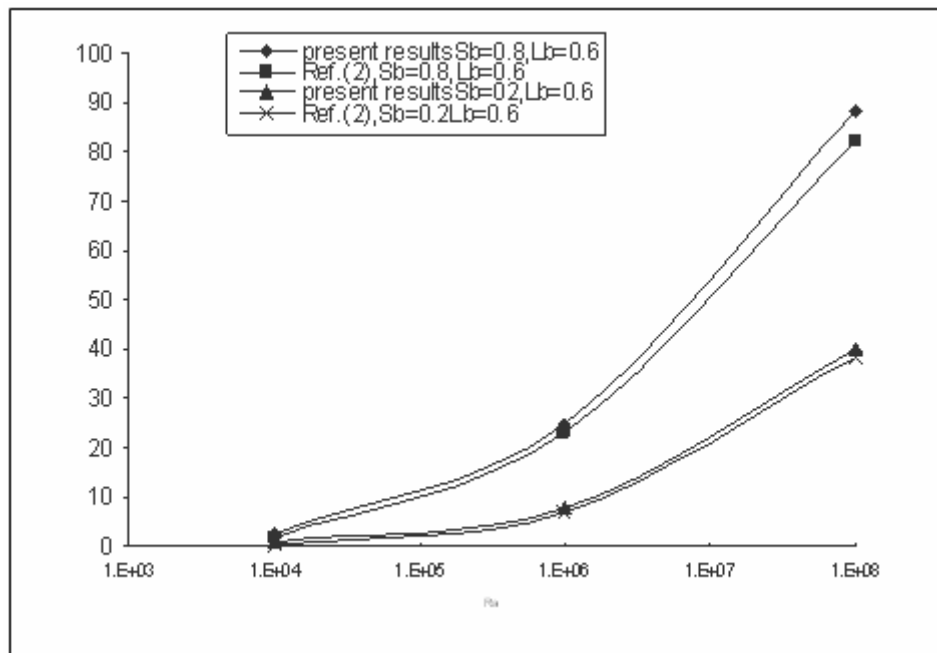


(b)

**Figure 8** Variation of Nusselt number with  $L_b$ ,  $S_b$  for  $A=1$ ; (a)  $S_b=0.2$ ,  $Ra=10^4$ , (b)  $L_b=0.6$ ,  $Ra=10^6$



(a)



(b)

**Figure 9** comparison of average Nusselt number and maximum absolute stream function with **Ref. [12]**